Available online at www.sciencedirect.com
SCIENCE DIRECT®
Journal of Solid State Chemistry 177 (2004) 895–900
JOURNAL OF SOLID STATE CHEMISTRY
http://elsevier.com/locate/jssc

The role of excess Zn^{2+} ions in improvement of red long lasting phosphorescence (LLP) performance of β-$Zn_3(PO_4)_2$:Mn phosphor

Jing Wang,[a] Shubin Wang,[a] and Qiang Su[a,b,*]

[a] *Key Laboratory of Rare Earth Chemistry and Physics, Changchun Institute of Applied Chemistry, Chinese Academy of Sciences, Changchun, Jilin 130022, People's Republic of China*

[b] *State Key Laboratory of Optoelectronic Materials and Technology, School of Chemistry and Chemical Engineering, Sun Yat-Sen University, Guangzhou 510275, People's Republic of China*

Received 4 July 2003; received in revised form 19 September 2003; accepted 24 September 2003

Abstract

Influences of excess Zn^{2+} ions and intrinsic defects on red ($\lambda = 616$ nm) phosphorescence of β-$Zn_3(PO_4)_2$:Mn^{2+} are systematically investigated. It is clearly observed that red long lasting phosphorescence (LLP) properties of Mn^{2+}, such as brightness and duration, are largely improved when excess Zn^{2+} ions are co-doped into the matrix. Photoluminescence (PL), LLP and thermoluminescence (TL) spectra indicate that Mn^{2+} ion acts as luminescent center whereas oxygen vacancy associated to Zn^{2+} ion plays a significant role in electron trap. The TL peak for oxygen vacancy is centered at 343 K, the depth of which is suitable for improvement in LLP performance of Mn^{2+} at room temperature. The possible mechanism for this phenomenon of red LLP of Mn^{2+} in β-$Zn_3(PO_4)_2$:Mn^{2+} with excess of Zn^{2+} is explained by means of a competitively trapping model.

Keywords: Zinc orthophosphate; Red long-lasting phosphorescence; Defects; Thermoluminescence; Competitively trapping model

1. Introduction

During the last decade, long lasting phosphorescence (LLP) materials have attracted much attention because they have large practical and potential applications in many fields, e.g., emergent lighting, display, detection of high-energy rays such as UV, X-ray, β-ray, etc., and multidimensional optical memory and imaging storage [1–4]. To the best of our knowledge, research interests worldwide have been mainly focused on rare earth ions, e.g. Ce^{3+}, Pr^{3+}, Tb^{3+} and especially Eu^{2+} [5–8]. Among them, most studies have been reported on commercial blue and green LLP materials, i.e., $CaAl_2O_4$:Eu^{2+},Nd^{3+}, $SrAl_2O_4$:Eu^{2+},Dy^{3+} [9–12]. The red LLP materials especially activated by Mn^{2+} ion remain to be explored.

Mn^{2+} ion should be expected as an efficient activator for red LLP materials since Mn^{2+} ion shows a high luminescence efficiency and a highly saturated color, and can be excited by almost all common excitation method, viz, X-ray, electron bombardment, UV-irradiation and electric field [13–15]. Indeed, Qiu et al. recently reported infrared femtosecond laser induced red LLP phenomenon in Mn^{2+} doped sodium borate glasses [16]. Thereafter, our group reported UV-induced red LLP with high performance in Mn^{2+} doped zinc borosilicate glasses [17], and Wang et al. observed red LLP phenomenon in $MgSiO_3$:Eu^{2+},Dy^{3+},Mn^{2+} [18].

In this paper, we first report red LLP phenomenon of Mn^{2+} in a phosphate matrix of polycrystalline β-$Zn_3(PO_4)_2$:Mn^{2+} in which traps with suitable depth and optimal concentration are successfully modified by introducing an excess of Zn^{2+} ions into β-$Zn_3(PO_4)_2$:Mn^{2+}. The red LLP of Mn^{2+} could be visible for about 2 h in the limit of light perception for naked eyes (0.32 mcd/m^2). The possible mechanism of this red LLP phenomenon in this matrix is explained by means of a competitively trapping model.

*Corresponding author. Key Laboratory of Rare Earth Chemistry and Physics, Changchun Institute of Applied Chemistry, Chinese Academy of Sciences, Changchun, Jilin 130022, People's Republic of China. Fax: +86-431-5698041.

E-mail address: suqiang@ciac.jl.cn, cessuq@zsu.edu.cn (Q. Su).

0022-4596/$ - see front matter © 2003 Elsevier Inc. All rights reserved.
doi:10.1016/j.jssc.2003.09.027

2. Experimental section

Powder samples were synthesized by solid-state reaction at high temperature. The raw materials were ZnO(A.G.), $(NH_4)_2HPO_4$(A.G.) and $MnCO_3$(A.G.). The concentration of Mn^{2+} ions was fixed to 2 mol% of the Zn ions in $3ZnO \cdot P_2O_5$, and the concentrations of excess Zn^{2+} ion were 0.5, 1.0, 2.0, 3.0 and 4.0 mol% of the Zn ions in $3ZnO \cdot P_2O_5$. The mixtures of corresponding raw materials were thoroughly grounded and then fired at 500°C for 3 h. After being reground, they were sintered at 950°C for 5 h in reducing atmosphere. The structure of all samples was analyzed by Rigaku D/max-IIB X-ray powder diffractometer using Cu$K\alpha_1$ ($\lambda = 1.5405$ Å) radiation and was coincident with β-$Zn_3(PO_4)_2$ (JCPDS: 30-1489).

Photoluminescence (PL) excitation and emission spectra were measured on a HITACHI F-4500 Spectrofluorometer equipped with monochromator (resolution: 0.2 nm) and 150 W Xe lamp. The LLP emission spectra and decay curves were detected as follows: immediately after being irradiated for 5 min by UV lamp peaking at 254 nm with a power of 4.07 mW/cm^2, the signal was recorded by the photomultiplier of HITACHI F-4500 Spectrofluorometer.

Thermoluminescence (TL) spectra were measured on FJ-427A TL meter (Beijing Nuclear Instrument Factory). Before measuring, powder samples were first pressed into pellets (5 mm in diameter and 0.5 mm in thickness), then sintered at 500°C under reducing atmosphere for the purpose of thermal bleaching, and finally exposed for 5 min to standard UV lamp peaking at 254 nm with a power of 4.07 mW/cm^2. The heating rate was fixed at 2 K/s within the temperature range from 293 to 773 K.

All measurements except TL spectra were performed at room temperature.

3. Results and discussion

3.1. The PL properties of $Zn_3(PO_4)_2$:$Mn^{2+}_{0.02}$ and $Zn_3(PO_4)_2$:$Mn^{2+}_{0.02}$ with excess 2 mol% Zn^{2+} ions

The free-ion levels for Mn^{2+}, in order of increasing energy, are ^{6}S, ^{4}G, ^{4}P, ^{4}D and ^{4}F, etc. However, influences of crystal field on electronic states of Mn^{2+} ($3d^5$) should be considered in detail when Mn^{2+} ion is doped in crystal. Orgel had calculated the diagram of energy level for Mn^{2+} ion in tetrahedral (CN = 4) or octahedral (CN = 6) crystal field, respectively. The designations in those environments are $^6A_{1g}$ (^{6}S), $^4T_{1g}$ (^{4}G), $^4T_{2g}$ (^{4}G), ^4E_g–$^4A_{1g}$ (^{4}G), $^4T_{2g}$ (^{4}D) and ^4E_g (^{4}D), etc. [19]. According to this diagram, the ^4E_g–$^4A_{1g}$ (^{4}G) and ^4E_g (^{4}D) levels are relatively of less influence than the others by crystal field. It means that the relative sharp lines can be expected in the absorption or excitation spectrum, which is usually used as the criterion for assignments of levels for Mn^{2+} ion.

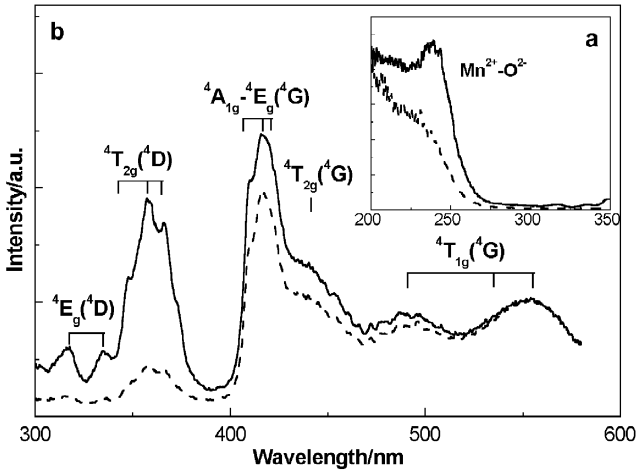

Fig. 1. The excitation spectrums of $Zn_3(PO_4)_2$:$Mn^{2+}_{0.02}$ (solid line) and 2 mol% Zn^{2+} rich-sample (dash line) at the wavelength from 200 to 300 nm (a), and from 300 to 580 nm (b).

In the present work, the excitation spectra of $Zn_3(PO_4)_2$:$Mn^{2+}_{0.02}$ and 2 mol% Zn-rich sample shown in Fig. 1, are divided into two parts. The first part consists of one broadband predominating around 240 nm as shown in Fig. 1a. It may be due to the charge transfer band of Mn^{2+}–O^{2-} [20], but not to host absorption because the edge of optical absorption band for $Zn_3(PO_4)_2$ is located at ~6.8 eV (182 nm) which is beyond the range of detection of our instruments [21]. The second part consists of several bands clearly shown in Fig. 1b, which are derived from the forbidden 3d–3d transitions of Mn^{2+} ion. Firstly, the two weak bands observed in the region from 300 to 340 nm, are components of the ^4E_g (^{4}D) levels. Then three bands in the region from 340 to 380 nm are assigned to the split $^4T_{2g}$ (^{4}D) levels, and three sharp bands at the wavelength from 400 to 430 nm are ascribed to the split $^4A_{1g}$, ^4E_g (^{4}G) levels. Finally, three broadbands are resolved in the region from 430 to 580 nm and assigned as components of the $^4T_{2g}$, $^4T_{1g}$ (^{4}G) levels. These assigned levels are mainly coincident with those reported by Palumbo and Brown [22].

In the emission spectra shown in Fig. 2a, one broadband predominates at 616 nm responding to the characteristic excitation band of Mn^{2+} at 418 nm. Under the UV light irradiation, Mn^{2+} ion is usually characterized by emitting green or red light. It consists of a d–d broadband corresponding to the transition of Mn^{2+} from the excited $^4T_{1g}$(^{4}G) state to the ground $^6A_{1g}$(^{6}S) state level. The emission color is strongly dependent on the coordination environment of Mn^{2+} in the host lattice, such as the coordination number (CN). The Mn^{2+} ion emits green light when it is tetrahedrally

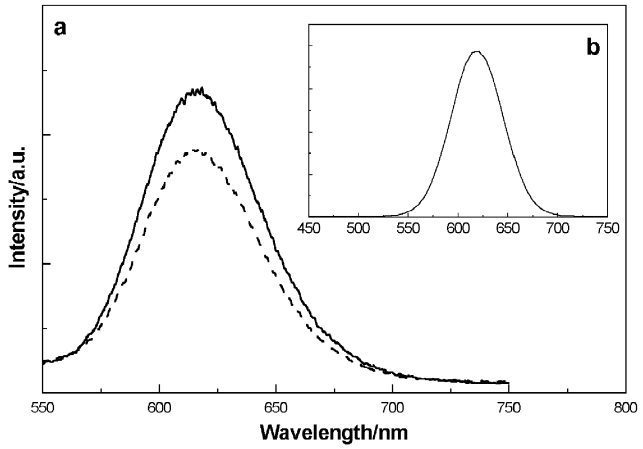

Fig. 2. The emission spectra (a) of $Zn_3(PO_4)_2$:$Mn^{2+}_{0.02}$ (solid line) and 2 mol% Zn^{2+} rich-sample (dashed line) under steady excitation at 418 nm, and LLP emission spectrum (b) of 2 mol% Zn^{2+} rich-sample after the removal of irradiation.

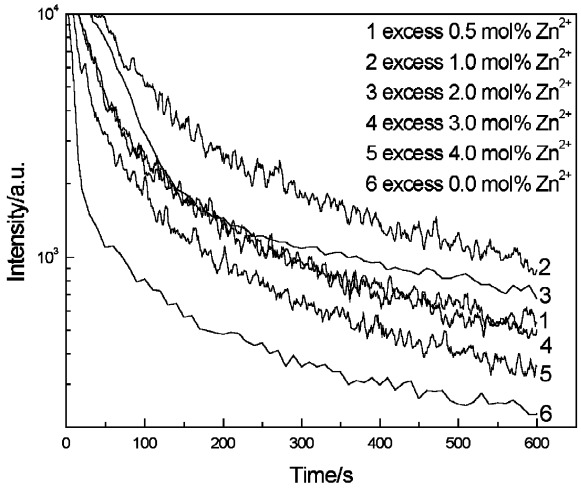

Fig. 3. The decay curves of $Zn_3(PO_4)_2$:$Mn^{2+}_{0.02}$ with excess x mol% Zn^{2+} ions monitored at 616 nm emission ($x = 0.0$, 0.5, 1.0, 2.0, 3.0 and 4.0).

coordinated (CN = 4) in the lattice, whereas it emits red light in octahedral coordination (CN = 6) [23]. In β-$Zn_3(PO_4)_2$, there are three non-equivalent cation sites, i.e., Zn(1), Zn(2) and Zn(3). Zn(1) and Zn(3) are bonded to four and five oxygen atoms, respectively, whereas Zn(2) is strongly bonded to five oxygen atoms and weakly bonded to an additional oxygen atom O(6) [24]. Therefore, the broad emission band peaking at 616 nm is assigned to the $^4T_{1g}(^4G) \rightarrow {}^6A_{1g}(^6S)$ transition of Mn^{2+} in the Zn(2) site with octahedral coordination (CN = 6).

From a careful comparison of excitation and emission spectra between two samples that are shown in Figs. 1 and 2a, it is found that excess 2 mol% Zn^{2+} ions decrease the emission intensity of Mn^{2+}. Generally, either intrinsic or foreign defects are harmful to efficient luminescence of activators since they could compete with activators and trap the excitation energy through non-irradiation transitions [25,26]. Therefore, excess Zn^{2+} ions, we think, may largely induce some intrinsic defects, such as oxygen vacancy, resulting in lower emission intensity of Mn^{2+}. This hypothesis will be largely supported by the following results.

After turnoff and removal of excitation source, the stoichiometric sample shows weak red LLP. Nevertheless, the introduction of excess 2 mol% Zn^{2+} ions induces improvement in red LLP performance of Mn^{2+} as shown in the decay curves 3 and 6 of Fig. 3. This red LLP can be observed for about 2 h in the limit of light perception for naked eyes (0.32 mcd/m^2). From inset in Fig. 2b, it is found that red LLP emission predominates around 616 nm, which is almost coincident with PL emission under steady excitation. It indicates that luminescence center for LLP is the same as that for PL which is derived from $^4T_{1g} \rightarrow {}^6A_{1g}$ transition of Mn^{2+} at Zn(2) site. Furthermore, the results mentioned above indicate that some intrinsic defects induced by excess Zn^{2+} ions may play a role in energy trapping under steady excitation. This reasonably explains why the emission intensity of Mn^{2+} in 2 mol% Zn^{2+} rich-sample is lower than that in stoichiometric sample $Zn_3(PO_4)_2$:$Mn^{2+}_{0.02}$ as shown in Fig. 2a. In addition, decay curves of these samples shown in Fig. 3 can be roughly divided into two parts, i.e., fast process and slow process.

3.2. *Defects properties of $Zn_3(PO_4)_2$:$Mn^{2+}_{0.02}$ with excess x mol% Zn^{2+} ions ($x = 0.0$, 0.5, 1.0, 2.0, 3.0, 4.0)*

The glow curves of stoichiometric and 2 mol% Zn^{2+}-rich samples are shown in Fig. 4a. Three peaks are clearly observed in stoichiometric sample. One peak predominates at 385 K, and the other two peaks are situated at 450 and 510 K, respectively. Furthermore, one shoulder, overlapped with and suppressed by the predominant peak at 385 K, is carefully observed around 343 K. For the sample with additional 2 mol% Zn^{2+} ions, one peak predominates at 343 K, and the other two shoulders dominate at 385 and 450 K, respectively.

With the careful comparison between glow curves shown in Fig. 4a, we think that there exist the same defects in the two samples, and that these defects may be mainly ascribed to the intrinsic defects in the host since they almost have the same peak position except TL intensity. For the peak at 343 K, the defect may be ascribed to oxygen vacancy that usually appears in the oxide host when a sample is sintered at reducing atmosphere [27,28]. In the stoichiometric sample, the amount of oxygen vacancy is relatively so fewer that the TL intensity of this peak is lower and suppressed by

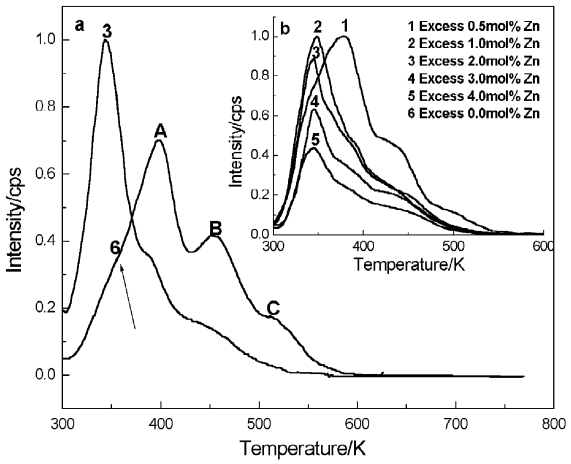

Fig. 4. TL spectra of $Zn_3(PO_4)_2$:$Mn^{2+}_{0.02}$ with excess x mol% Zn^{2+} ions ($x = 0.0$, 0.5, 1.0, 2.0, 3.0 and 4.0).

the predominant peak at 385 K as shown in the glow curve 6 of Fig. 4a. When the excess Zn^{2+} ions are doped into the host, the chemical composition of the sample deviates from the stoichiometric ratio, i.e., Zn/P > 3:2. From the viewpoint of the defects chemistry, this means that a few of the oxygen atoms normally coordinated to zinc atom are absent. That is to say, the defect of oxygen vacancy would appear around the site of Zn^{2+} [29,30]. Therefore, more oxygen vacancies would be created due to excess Zn^{2+} ions, resulting in enhancement of TL intensity of the peak at 343 K. Indeed the enhancement of TL intensity of the peak at 343 K is clearly observed in glow curve 3 of Fig. 4a. For peaks above 343 K, it seems too difficult to identify the nature of them. Thus, these peaks at 385, 450 and 510 K here are temporarily noted as defect A, B and C, respectively, since they do not influence discussions about red LLP performance of Mn^{2+} in the present sample.

3.3. The possible mechanism of red LLP of Mn^{2+} in $Zn_3(PO_4)_2$:Mn^{2+} with excess Zn^{2+} ions

In the following, the possible mechanism of red LLP of Mn^{2+} in β-$Zn_3(PO_4)_2$ will be discussed in detail. A competitively trapping model is proposed to interpret the significant role of excess Zn^{2+} ions in the improvement of red LLP of Mn^{2+} in β-$Zn_3(PO_4)_2$ based on those results mentioned above. Furthermore, additional experiments are being designed and carried out.

Under UV excitation, electrons and holes are generated. The holes are captured by Mn^{2+} ions that result in the excited state of Mn^{2+} ions, $(Mn^{2+})^*$ [31,32], and the electrons are competitively captured at the traps of oxygen vacancies, as-expressed defects A, B or C. The distribution of electrons at these defects above is different which directly reflects the different ability of trapping electrons by these defects. From Fig. 4, it can be seen that such ability for trapping oxygen vacancy seems to be higher. Subsequently, electrons trapped at these defects are thermally released and finally recombine with $(Mn^{2+})^*$ at room temperature, resulting in the phenomenon of red LLP of Mn^{2+} as shown in Fig. 2b.

Based on this possible model mentioned above, we think two aspects of oxygen vacancy induced by excess Zn ion, i.e., the trap depth and its concentration, are responsible for improvement of red LLP performance of Mn^{2+}.

The first one is trap depth of oxygen vacancy. Usually, information of traps distribution can be obtained by TL measurements. The shallower the charge trap is, the lower the temperature of TL peak is [33]. For LLP material, one significant factor is the suitable trap depth that is related to temperature of TL peak [12,34,35]. If the depth of electron trap is too deep, the electrons will be strongly bound at the trap. On the contrary, if the depth of electron trap is too shallow, the electrons will be more easily released from the trap. Therefore, both traps mentioned above do not contribute to the LLP. To the best of our knowledge, the predominant peak is situated slightly above room temperature if materials show high LLP performance [1,8,12]. Therefore, the peak at 343 K, induced by oxygen vacancy, is preferred as the electron trap with suitable depth responsible for improvement of red LLP performance of Mn^{2+} ion in the present sample. In the stoichiometric sample, the amount of defect A is relatively larger than that of oxygen vacancy from the viewpoint of defects distribution as shown in curve 6 of Fig. 4a. Hence, most electrons are competitively captured by defect A with deeper depth instead of oxygen vacancy, resulting in high TL intensity of the peak at 385 K and poor performance of red LLP of Mn^{2+}. However, Zn^{2+} ions in excess of 2 mol% results in increasing amount of oxygen vacancy and therefore induces enhancement of TL intensity of the peak at 343 K, which is clearly indicated in glow curve 3 of Fig. 4a. The increasing amount of oxygen vacancy directly results in the increasing of its ability for trapping electrons compared to the other intrinsic defects, especially defect A. Thus, most electrons are trapped at oxygen vacancy in the procedure of competitively trapping. And the improvement of red LLP performance of Mn^{2+} is clearly observed in the decay curve 3 of Fig. 3.

Another factor is concentration of electron trap, i.e., oxygen vacancy in the present samples. Generally, the amount of electrons captured at the trap, which is proportional to that of the electron trap under the optimal concentration, can determine the LLP property if the depth of the electron trap is kept constant [8,12]. Thus the increasing amount of electron trap will result in the improvement of LLP to some extent. For the purpose of confirming this hypothesis, a series of

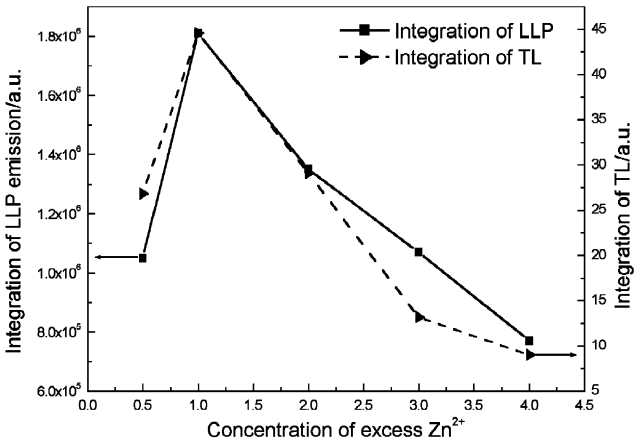

Fig. 5. The intensity integrations of LLP ($E_m = 616$ nm) within 600 s and of TL ($T_{max} = 343$ K) vs. concentration of excess Zn^{2+}.

samples doped with excess Zn^{2+} ions was prepared. The decay and glow curves are measured under the same condition. These results are shown in Figs. 3 and 4b, respectively. The LLP emission at 616 nm is integrated within 600 s, and TL peaking at 343 K is also integrated after those glow curves are deconvoluted. Fig. 5 summarizes relationships between integrated value and the concentration of excess Zn^{2+} ions.

From Fig. 4b, it is clearly observed that the position of two major peaks at 343 and 385 K does not change the concentration of excess Zn^{2+} ions as increases. This indicates that the chemical nature of defects related to these two peaks is not changed, which is ascribed to oxygen vacancy and intrinsic defect A for peaks at 343 and 385 K, respectively. When additional 0.5 mol% Zn^{2+} ions are doped into the host, the predominant peak is still situated at 385 K, and the improvement of red LLP performance of Mn^{2+} is also observed in decay curve 1 of Fig. 3. This is reasonably explained by the simultaneous increase of the amount of oxygen vacancy corresponding to the shoulder peak at 343 K as shown in curve 1 of Fig. 4b. As the concentration of excess Zn^{2+} ions is equal to and upto 1 mol%, the peak at 343 K is predominant and suppressed the other peaks (A, B and C). Therefore, the improvement of red LLP is naturally expected in Figs. 3 and 5. Additionally, it is clearly observed from Figs. 4b and 5 that TL intensity of the peak at 343 K first increases as the amount of excess Zn^{2+} ions is up to 1 mol%, and then decreases as the amount of excess Zn^{2+} ions further increases. Such concentration effects are ascribed to the relationship between retrapping probability and concentration of oxygen vacancy. The retrapping probability may be negligible in the region of lower concentration, and becomes predominant in the region of higher concentration. This phenomenon is similar to the concentration quenching of activator in the field of PL, which is due to the reabsorption of the activator.

4. Conclusions

The red LLP of Mn^{2+} is reported in phosphate matrix of polycrystalline β-$Zn_3(PO_4)_2$:Mn^{2+} for the first time. Influences of excess Zn^{2+} ions and intrinsic defects on red LLP performance of β-$Zn_3(PO_4)_2$:Mn^{2+} have been systematically investigated. The optimal concentration of excess Zn^{2+} ions for the improvement of red LLP performance of Mn^{2+} is nominally 1 mol% of Zn ions in $3ZnO \cdot P_2O_5$:$Mn^{2+}_{0.02}$. After the removal of irradiation source, the red LLP of Mn^{2+} predominant at 616 nm can be visible for about 2 h in the limit of light perception for naked eye (0.32 mcd/m^2). The TL peak situated at 343 K is assigned to oxygen vacancy, a significant electron trap responsible for improvement of red LLP of Mn^{2+} in the present matrix. The possible mechanism of this red LLP phenomenon in this matrix has been explained by means of a competitively trapping model.

Acknowledgments

We are very grateful to State Key Project of Basic Research (G1998061312) of China for financial support.

References

[1] T.Z. Zhang, Q. Su, J. SID. 8 (2000) 27–30.
[2] M. Kowatari, D. Koyama, Y. Satoh, K. Iinuma, S. Uchida, Nucl. Instrum. Methods Phys. Res. A 480 (2002) 431–439.
[3] J. Qiu, K. Miura, H. Inouye, Appl. Phys. Lett. 73 (1998) 1763–1765.
[4] C.Y. Li, Y.N. Yu, S.B. Wang, Q. Su, J. Non-Crystal. Solids 321 (2003) 191–196.
[5] N. Kodama, T. Takahashi, M. Yamaga, Appl. Phys. Lett. 75 (1999) 1715–1717.
[6] S.X. Lian, J.H. Lin, M.Z. Su, Chin. J. Rare Earth 19 (2001) 602–605.
[7] T. Kinoshita, M. Yamazaki, H. Kawazoe, J. Appl Phys. 86 (1999) 3729–3733.
[8] T. Matsuzawa, Y. Aoki, N. Takeuchi, J. Electrochem. Soc. 143 (1996) 2670–2673.
[9] H. Yamamoto, T. Matsuzawa, J. Lumin. 72–74 (1997) 287–289.
[10] K. Kato, I. Tsutai, T. Kamimura, J. Lumin. 82 (1999) 213–220.
[11] W. Jia, H. Yuan, L. Lu, J. Lumin. 76–77 (1998) 424–428.
[12] T.Z. Zhang, Q. Su, S.B. Wang, Chin. J. Lumin. 20 (1999) 170–175.
[13] B.A. Smith, J.Z. Zhang, Phys. Rev. B 62 (2000) 2021–2028.
[14] T. Minami, T. Maeno, Y. Kuroi, S. Takata, Jpn. J. Appl. Phys. 34 (1995) L684–L687.
[15] L.E. Shea, R.L. Datta, J.J. Brown, J. Electrochem. Soc. 141 (1994) 1950–1954.
[16] J.R. Qiu, Y. Kondo, K. Miura, T. Mitsuyu, K. Hirao, Jpn. J. Appl. Phys. 38 (1999) L649–L651.

[17] C.Y. Li, S.B. Wang, Q. Su, Mater. Res. Bull. 37–38 (2002) 1443–1449.
[18] X.J. Wang, D.D. Jia, W.M. Yen, J. Lumin. 102–103 (2003) 34–37.
[19] L.E. Orgel, J. Chem. Phys. 23 (1955) 1004–1014.
[20] J. Lin, D.U. Sanger, M. Mennig, K. Barner, Thin Solid Films 360 (2000) 39–45.
[21] J.K. Berkowitz, J.A. Olsen, J. Lumin. 50 (1991) 111–121.
[22] D.T. Palumbo, J.J. Brown, J. Electrochem. Soc. 117 (1970) 1184–1188.
[23] S. Linwood, J. Wegl, J. Opt. Soc. Am. 42 (1952) 910–916.
[24] J.S. Stephens, C. Calvo, Can. J. Chem. 45 (1967) 2303–2312.
[25] W.V. Schaik, G. Blasse, Chem. Mater. 4 (1992) 410–415.
[26] W. Kostler, A. Winnacker, W. Rossner, B.C. Grabmaier, J. Phys. Chem. Solids 56–57 (1995) 907–913.
[27] H. Hosono, T. Kinoshita, H. Kawazoe, M. Yamazaki, Y. Yamamoto, N. Sawanobori, J. Phys. Condens. Matter 10 (1998) 9541–9547.
[28] J. Qiu, K. Hirao, Solid State Commun. 106 (1998) 795–798.
[29] G. Hong, Inorganic Solid State Chemistry, Sciences Press, Beijing, 2002.
[30] J.P. Han, P.Q. Mantas, A.M.R. Senos, J. Euro. Ceramic Soc. 22 (2002) 49–59.
[31] C.Y. Li, Q. Su, J. Qiu, Chin. J. Lumin. 24 (2003) 19–27.
[32] M. Iwasaki, D.N. Kim, K. Tanaka, T. Murata, K. Morinaga, Sci. Tech. Adv. Mater. 4 (2003) 137–142.
[33] S.W.S. Mckeever, R. Chen, Radiat. Meas. 27 (1997) 625–661.
[34] D. Haranath, V. Shanker, H. Chander, P. Sharma, Mater. Chem. Phys. 78 (2002) 6–10.
[35] A. Nag, T.R.N. Kutty, J. Alloys Compounds 354 (2003) 221–231.